

CFD Analysis and Optimization Dimension on the Snubber with buffer of Reciprocating Hydrogen Compressor

왕복동식 수소압축기에서 버퍼가 있는 스너버의 수치해석 검증과 최적의 크기 도출

G. H. Lee, W. A. Akbar, K. J. Shim, H. Min. Jeong and H. S. Chung
이경환 · 악바르 · 심규진 · 정한식 · 정효민

Key Words : Hydrogen Gas(수소가스), Reciprocating Compressor(왕복동식 압축기), Pulsation Pressure, Fluctuation(맥동압), Snubber(스너버), Buffer(버퍼)

요약 : 수소 추출과 리포밍 과정, 연료 전지, 저장소로 구성된 수소 연료에 대한 연구는 세계적으로 번영하고 있는 중이다. 그러나 한국의 수소 스테이션에 대한 연구는 아직도 개발이 미미한 수준이다. 그리고 역시 수소 스테이션의 가장 중요한 부분인 수소 압축기에 대한 연구도 미흡하다. 수소압축기에서 가장 중요한 부분 중에 하나는 스너버인데 이것의 기능은 수소가스의 맥동압을 줄이고 불순물을 제거한다. 스너버 내부에는 버퍼라고 불리는 기울어진 판이 설치되어 맥동압을 줄이고 불순물을 제거하는 역할을 담당한다. 스너버 내부의 압력 손실과 맥동압이 최소가 될 때 스너버는 적절한 성능을 가졌다고 평가된다. 그러므로 이 연구의 목적은 수치해석을 통하여 스너버의 최적의 기하학적 크기와 버퍼의 각도에 따른 최적의 스너버를 찾는 것이다. 수치해석의 결과에서 다양한 버퍼각도에 따른 스너버의 독특한 특성을 볼 수 있다. 결과적으로 버퍼의 각도가 35°일때 최소의 압력손실이 발생했고, 버퍼의 각도가 10°일 때 최소의 맥동압이 발생하였다.

NOMENCLATURE

- P_{TL} : total pressure loss [Pa=N/m²]
- P_F : pressure pulsation [Pa]
- P_{mean} : mean pressure value [Pa]

1. INTRODUCTION

The use of hydrogen as a transport fuel has been investigated for a few decades, but in the past 10 years the number of research and pilot projects has escalated. The recent hikes in the price of oil have also added impetus to the movement towards hydrogen and other

alternatives fuels¹⁾.

A methodology for the integrated production planning and reactive scheduling in the optimization of a hydrogen supply network was proposed by SA. Heever et al in²⁾. In this network's model, compressing system takes an important part of whole system. Generally, hydrogen compressor is reciprocating two-stage type. The schematic drawing of the real Hydrogen compressing system is shown by Fig. 1. From that figure, the snubbers applied to each compressor stage can be seen clearly. Here, four units of snubber are used for each inlet and outlet for the first and second stage.

Technically reciprocating compressor type has higher pressure ratio than the rotating one. Therefore this type is used in hydrogen handling both for storing and transferring. Special character of pressure produced by this compressor

접수일 : 2008년 5월 29일, 채택확정 : 2007년 10월 9일
정한식(책임저자):경상대학교 정밀기계공학과,해양산업연구소
E-mail : hschung@gnu.ac.kr, Tel : 055-646-4766
이경환, 악바르, 심규진 : 경상대학교 대학원 정밀기계공학과
정효민 : 경상대학교 정밀기계공학과, 해양산업연구소

is pulsation or fluctuation. This phenomenon has a lot of disadvantages not only for the gas itself but also for equipments relating to the system. For this occasion the snubber was designed and used³⁾. In order to damp the pressure fluctuation a flat plate is inserted inside the snubber. This plate is called buffer. The installation of a buffer inside a snubber can be seen in the cutting view in Fig 2. An experiment to find out the effect of buffer presence in a snubber had already been conducted⁴⁾. This resulted a fact that snubber with buffer has better performance. As addition, the design of pulsation and vibration control for hydrogen compressor system should consider requirements in the API Standard 618 book⁵⁾.

For several parameters in low pressure range, hydrogen gas has same character with the atmosphere air. Especially to observe the pressure from physical approach (without considering the chemical character), pressured air can be used to represent hydrogen gas. Modeling hydrogen compressor by using air compressor unit brought a good agreement with the CFD simulation. After

that, the study was focus on the numerical analysis to achieve the optimum dimension for snubber. This paper explains about the effect of varying buffer angle to the pressure characteristics. Three models group, distinguished with the volume, are compared.

2. EXPERIMENTAL SETUP AND METHOD

Experiment was done to observed pressure characteristic flow trough a snubber. So the devices were installed like Fig. 3. A snubber placed in the middle of pipe lines. One of the pipe is function as inlet, so it was connected to the compressor. And the other pipe is function as outlet to release the pressured gas.

Two units of pressure sensor was placed at inlet and outlet point as shown by Fig. 4. For with-buffer snubber, a flat plate is located inside the snubber.

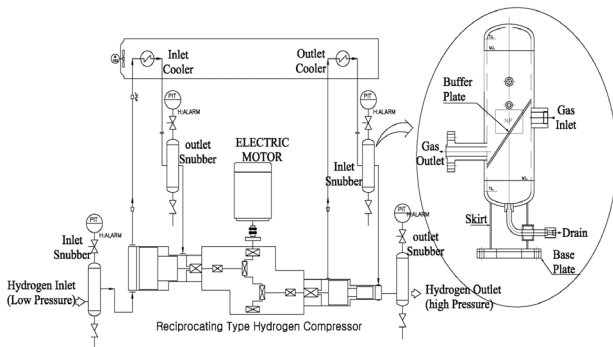


Fig. 1 Schematic diagram of a hydrogen gas compressing system



Fig. 2 Detailed and cutting view of a snubber

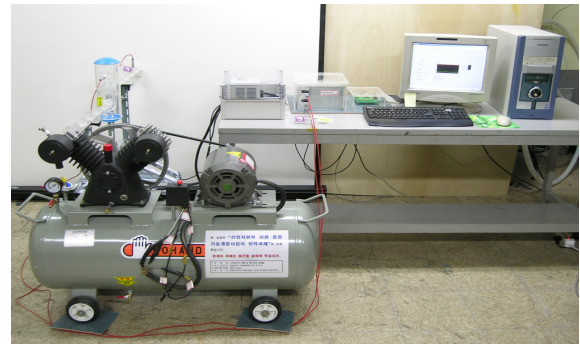


Fig. 3 Experimental setup

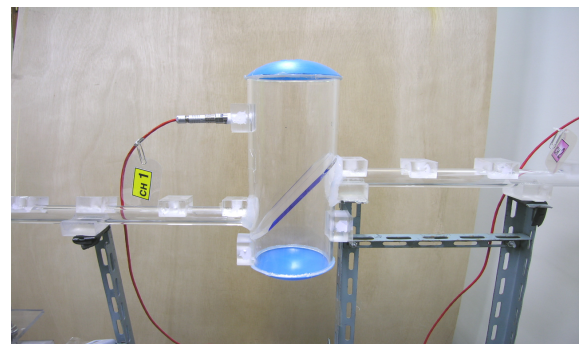


Fig. 4 Sensors position

Experiment conducted by running the compressor and setting motor frequency at six

values. These are 10, 20, 30, 40, 50 and 60 Hz. Pressure value is sensed by pressure sensor, amplified and recorded in a PC.

3. NUMERICAL ANALYSIS AND METHOD

The purpose of deriving mathematical model in CFD is to find the appropriate relation between each fluid flow properties. The three dimensional, compressible, turbulent flow of the gas in the test problems is governed by partial differential equations that express the principles of conservation of mass, momentum and energy. In this paper, the turbulent model chosen was k-ε with high Reynolds number. All of these equations below were taken from Star CD's, the CFD code used, Methodology book⁽⁶⁾.

The continuity equation

$$\frac{\partial \rho}{\partial t} + \frac{\partial(\rho U)}{\partial x} + \frac{\partial(\rho V)}{\partial y} + \frac{\partial(\rho W)}{\partial z} = 0$$

x-direction momentum equation

$$\begin{aligned} & \frac{\partial(\rho U)}{\partial t} + \frac{\partial(\rho U^2)}{\partial x} + \frac{\partial(\rho UV)}{\partial y} + \frac{\partial(\rho UW)}{\partial z} \\ & - \frac{\partial}{\partial x} \left(\mu_{eff} \frac{\partial U}{\partial x} \right) - \frac{\partial}{\partial y} \left(\mu_{eff} \frac{\partial U}{\partial y} \right) - \frac{\partial}{\partial z} \left(\mu_{eff} \frac{\partial U}{\partial z} \right) \\ & = - \frac{\partial P}{\partial x} + S^U \end{aligned}$$

y-direction momentum equation

$$\begin{aligned} & \frac{\partial(\rho V)}{\partial t} + \frac{\partial(\rho UV)}{\partial x} + \frac{\partial(\rho V^2)}{\partial y} + \frac{\partial(\rho VW)}{\partial z} \\ & - \frac{\partial}{\partial x} \left(\mu_{eff} \frac{\partial V}{\partial x} \right) - \frac{\partial}{\partial y} \left(\mu_{eff} \frac{\partial V}{\partial y} \right) - \frac{\partial}{\partial z} \left(\mu_{eff} \frac{\partial V}{\partial z} \right) \\ & = - \frac{\partial P}{\partial y} + S^V \end{aligned}$$

z-direction momentum equation

$$\begin{aligned} & \frac{\partial(\rho W)}{\partial t} + \frac{\partial(\rho UW)}{\partial x} + \frac{\partial(\rho VW)}{\partial y} + \frac{\partial(\rho W^2)}{\partial z} \\ & - \frac{\partial}{\partial x} \left(\mu_{eff} \frac{\partial W}{\partial x} \right) - \frac{\partial}{\partial y} \left(\mu_{eff} \frac{\partial W}{\partial y} \right) - \frac{\partial}{\partial z} \left(\mu_{eff} \frac{\partial W}{\partial z} \right) \\ & = - \frac{\partial P}{\partial z} + S^W \end{aligned}$$

Turbulence kinetic energy equation

$$\begin{aligned} & \frac{\partial(\rho k)}{\partial t} + \frac{\partial(\rho Uk)}{\partial x} + \frac{\partial(\rho Vk)}{\partial y} + \frac{\partial(\rho Wk)}{\partial z} \\ & - \frac{\partial}{\partial x} \left\{ \left(\frac{\mu_t}{\sigma_k} + \mu \right) \frac{\partial k}{\partial x} \right\} - \frac{\partial}{\partial y} \left\{ \left(\frac{\mu_t}{\sigma_k} + \mu \right) \frac{\partial k}{\partial y} \right\} \\ & - \frac{\partial}{\partial z} \left\{ \left(\frac{\mu_t}{\sigma_k} + \mu \right) \frac{\partial k}{\partial z} \right\} \\ & = G_k - \rho \epsilon \end{aligned}$$

turbulence dissipation rate equation

$$\begin{aligned} & \frac{\partial(\rho \epsilon)}{\partial t} + \frac{\partial(\rho U \epsilon)}{\partial x} + \frac{\partial(\rho V \epsilon)}{\partial y} + \frac{\partial(\rho W \epsilon)}{\partial z} \\ & - \frac{\partial}{\partial x} \left\{ \left(\frac{\mu_t}{\sigma_\epsilon} + \mu \right) \frac{\partial \epsilon}{\partial x} \right\} - \frac{\partial}{\partial y} \left\{ \left(\frac{\mu_t}{\sigma_\epsilon} + \mu \right) \frac{\partial \epsilon}{\partial y} \right\} \\ & - \frac{\partial}{\partial z} \left\{ \left(\frac{\mu_t}{\sigma_\epsilon} + \mu \right) \frac{\partial \epsilon}{\partial z} \right\} \\ & = C_1 \frac{\epsilon}{k} G_k - C_2 \rho \frac{\epsilon^2}{k} \end{aligned}$$

$$G_k = \mu_t \cdot \left[\left(\frac{\partial u}{\partial y} + \frac{\partial v}{\partial x} \right)^2 + \left(\frac{\partial v}{\partial z} + \frac{\partial w}{\partial y} \right)^2 + \left(\frac{\partial w}{\partial x} + \frac{\partial u}{\partial z} \right)^2 \right]$$

3.1 Pressure Characteristics Analysis

The main functions of the snubber are to reduce the pulsation and (in the same time) to keep the pressure magnitude. For that reason, three following equations are derived.

$$P_{TL} = \frac{\Delta P}{P_{in}} \times 100\% \quad (1)$$

$$P_F = \sum \frac{\Delta P}{2 \times P_{mean}} \times 100\% \quad (2)$$

In these equations, ΔP , P_{in} , P_{out} , P_{TL} , P_F and P_{mean} are pressure difference, inlet pressure, outlet pressure, total pressure loss, pressure pulsation and mean pressure value, respectively. Reducing the pulsation means reducing P_F value, while keep the pressure magnitude means keep P_{TL} value as low as possible.

3.2 Computational Methodology

The computational code used was Star CD (Version 3.24), which solve the full 3D time dependent Navier-Stokes, continuity and energy

equations using the finite volume method. This commercial code is widely used in the numerical simulation of different flow conditions in various complex geometries and was chosen in this study because it is proven capability and validity. The turbulent flow in this investigation is considered to be transient, incompressible, viscous, Newtonian and isotropic.

The numerical solution involves splitting the geometry into many sub-volumes and then integrating the differential equations over these volumes to produce a set of coupled algebraic equations for the velocity components, and the pressure at the centre of each volume. The solver guesses the pressure field and then solves the discretion form of the momentum equations to find new values of the pressure and velocity components. This process continues, in iterative manner, until the convergence criterion is satisfied. In this study, simulation was started by verifying the numerical result to the experimental result. It has been done and gave good agreement. Afterward the simulation series for different snubber model was conducted (section 5).

3.3 Modeling and Grid System

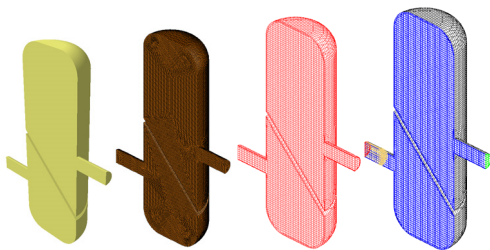


Fig. 5 Computational model: (a) 3D design, (b) Surface mesh in pro-surf, (c) Volume mesh and (d) Boundary condition

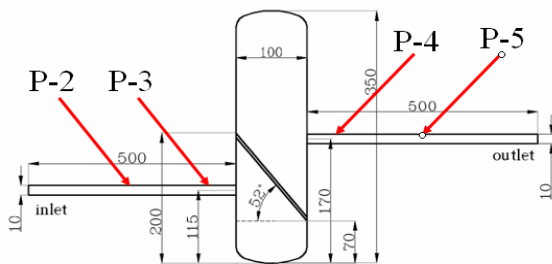


Fig. 6 Dimension of computational model with observed point positions

3.4 Boundary Condition and verification of the Computational Method

In order to solve the partial differential equations described in section 3, appropriate boundary conditions must be declared for all boundaries of the computational domain. The boundary conditions associated with the computational domain as shown in fig. 5(d) are inflow, outflow and symmetry plane. In order to reduce the cell number and the calculation time also, the model was made in a half type. This is regarding the symmetrical shape of the snubber. Therefore the symmetry boundary condition was applied on the cross section marked by blue color in fig. 5(d).

The inflow was set to the pressure value taken from measured data from the experiment. The data is transient and waving with maximum and minimum limit. The pressure value is different for each motor frequency.

Fig. 7, 8 and 9 shows the inflow data as the boundary condition for motor frequency 20, 40 and 60 Hz. Boundary condition for the outflow was set to the atmospheric pressure value, 101.325 kPa. The dimension of the model is depicted in Figure 6. In this figure the four points where the sensors were placed also are pointed. So the corresponding location in the CFD model must be the observing objects. The simulation was run for three simulations, according to different motor frequency. The mean pressure for the measuring points was compared. From the data the comparison graph can be plotted as fig. 10, 11 and 12. All of those three graphs show the same trend between CFD and experimental result.

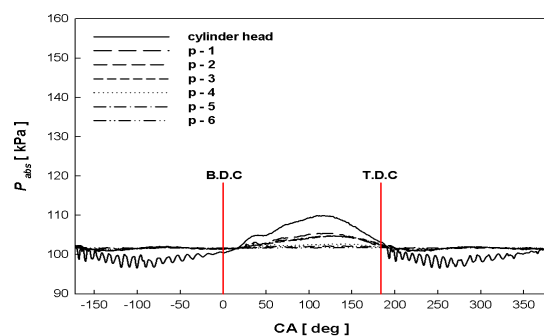


Fig. 7 Pressure fluctuation through snubber for motor frequency at 20 Hz

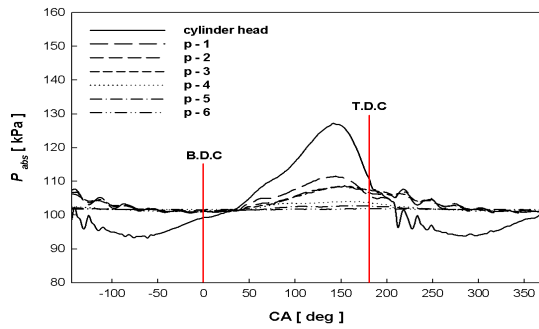


Fig. 8 Pressure fluctuation through snubber for motor frequency at 40 Hz

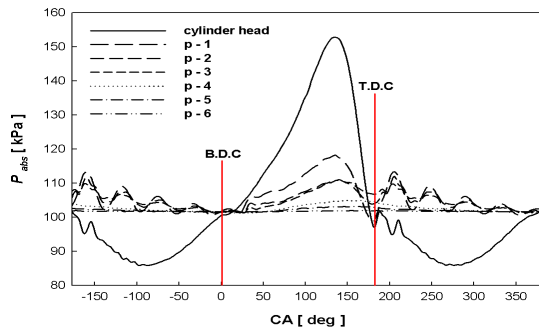


Fig. 9 Pressure fluctuation through snubber for motor frequency at 60 Hz

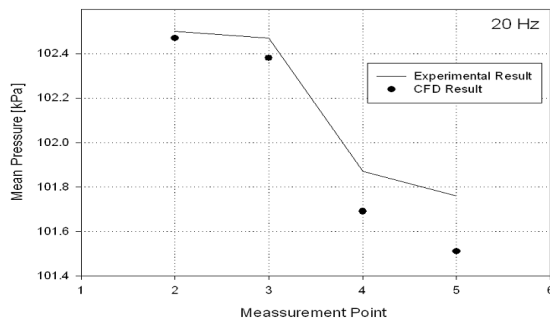


Fig. 10 Comparison of numerical with experimental data at 20 Hz

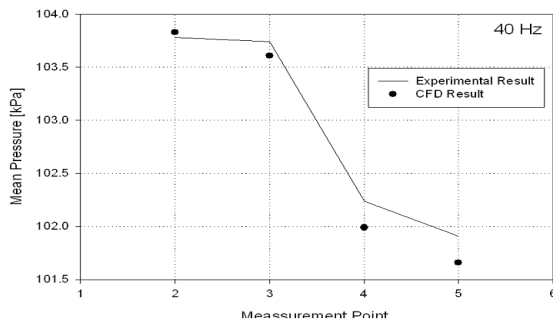


Fig. 11 Comparison of numerical with experimental data at 40 Hz

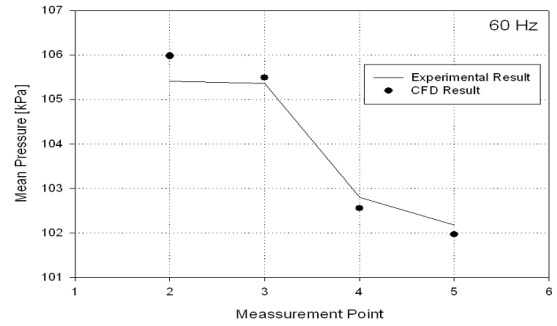


Fig. 12 Comparison of numerical with experimental data at 60 Hz

4. SIMULATION FOR VARIOUS SNUBBER TYPES

The appropriate modeling and simulation setting described in previous discussion are the basic to extend the investigation for various dimensions of snubber. The purpose is to find the optimum design of it. In designing a snubber several dimension such as snubber height (H), snubber diameter (D), buffer width (W) and buffer angle (θ) must be defined. Fig. 13 illustrates all of dimensions mentioned above. The simulation run in this paper were occupying three groups of snubber volume, they are $H/D = 3.23$, $H/D = 3.82$ and $H/D = 4.48$. The volume size for each models are 0.0124mm^3 , 0.0147mm^3 and 0.0170mm^3 respectively. The complete dimension parameters are listed in table 1. Each model requires specific grid system shown in figure 14.

Like as the simulation to get verified data, the trimmed-hexagonal cell also was used. The half-symmetry model was used to reduce the cell number.

Therefore the calculation job will be reduced. Special treatment was applied to the area near the wall. In these areas the mesh size was made much smaller, so the accurate calculation should be made. Fig. 14(d) shows the detailed view of cross section of the model.

This work was to solve the real problem occurred in the hydrogen gas station. Therefore in this simulation the real dimension and condition are use. The model with $H/D = 3.82$

with 0.0147 mm^3 is the one which is used in the industry field, in this paper this is named as standard model.

Two other models are studied as the benchmarks. One model has volume bigger than the standard model and the other has smaller than the standard. To produce the comparable result to the real condition, so the boundary condition, material properties and numerical setting were adjusted to approach the reality. The inlet pressure for boundary condition was set to the high enough value representing the operational pressure in the real hydrogen gas plant. This mean pressure value was stated of 10 MPa with pulsation factor of 2 MPa. Fig. 15 shows this inlet boundary condition. On the other hand, the pressure outlet boundary condition was set of non pulsating 10 MPa. Hydrogen gas properties applied into this computation were taken from Star CD material database. The computation was set with transient condition, compressible flow and using $k-\epsilon$ high Reynolds number turbulent model. Upwind scheme was chosen to execute the calculation for all variables, such as mass, U, V, W momentum, pressure and turbulent kinetic energy.

The study is focused on pressure at point 1 and point 2 in the fig. 16. These measured points, both at inlet and outlet pipe, are located 50 mm from the snubber wall. These points were chosen in order to analyze damping phenomena inside the snubber.

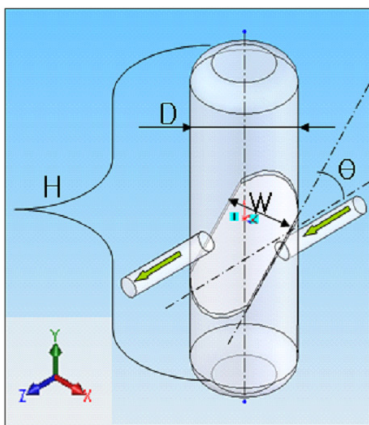


Fig. 13 Modeling notifications

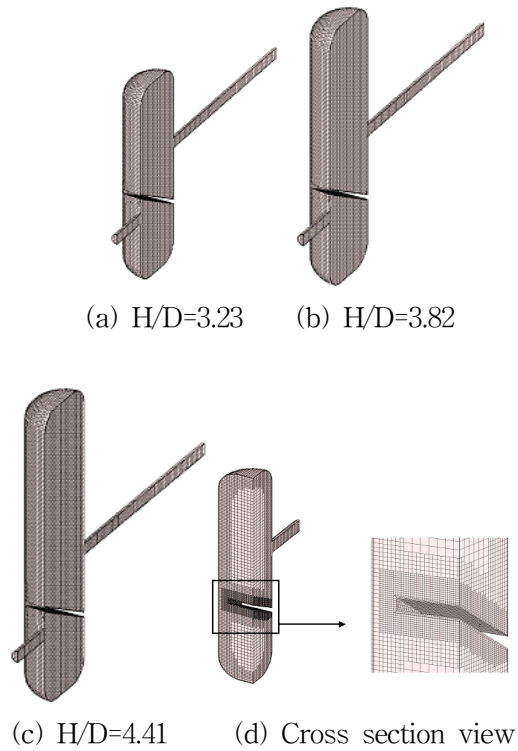


Fig. 14 Grid systems of the models

5. RESULT AND DISCUSSION

The simulation result the mean pressure value at point 1 and point 2. The mean pressure at point 1 is shown by fig. 17, meanwhile at point 2 by fig. 18. At point 1, inlet pipe, the mean pressure decrease as the increasing snubber volume. For all snubber volume models, the trends are quite similar based on varying buffer angle. For $H/D = 3.23$, start from 10 deg up to 30 deg, the pressure quite constant. And start to increase when $\theta = 30$ deg until 50 deg. For $H/D = 3.82$, start from 10 deg up to 35 deg, the pressure quite constant. Then start to increase when $\theta = 35$ deg until 50 deg. The unique occurred in $H/D = 4.41$, when pressure decline from 10 deg until 25 deg and incline smoothly from 25 deg until 35 deg then drastically from 35 deg to 50 deg. Pressure in the without buffer model is bigger than pressure with 45 deg buffer for all models. At point 2, outlet pipe, the mean pressure also indicates a unique pattern. All models show smooth increasing from 10 deg until 50 deg.

Applying equation (1) and (2), fig. 19 and fig.

20 can be made. These two graphs depict the objective functions. As known before P_{TL} and P_F are the pressure characteristics those are become optimization parameters. The goal of this optimization is to minimize both of those values. As can be seen in fig. 19, P_{TL} is increasing as the increasing snubber volume. All models show curved-like trend with minimum value at 35 deg. For $H/D = 3.82$ and $H/D = 4.41$, the value decline smoothly start from 10 deg until 35 deg, after that incline with very small changes. And for $H/D = 3.23$, the value decline smoothly start from 10 deg until 40 deg, after that incline up to 50 deg.

The P_F is increasing from 10 deg until 50 deg for all models. According to the fact discussed above the optimization face a problem where the minimum value for both parameters is not occurred at the same buffer angle. Therefore the advance study to determine optimum value must be developed. This should consider not only minimizing mean pressure loss and pressure pulsation but also minimizing the snubber volume.

Table 1 Geometrical data for various snubber models

Parameters (mm)	H/D 3.23	H/D 3.82	H/D 4.41
Diameter	170		
Height	550	650	750
Inlet Pipe Diameter	30		
Outlet Pipe Diameter	30		
Inlet Pipe Length	100		
Outlet Pipe Length	500		
Inlet Pipe Position Form Bottom	175		
Outlet Pipe Position Form Bottom	310		
Width	60		
Thickness	10		
Angle	10°~50°(increase with 5°)		
(m ³)	0.0124	0.0147	0.0170
Grid Cells Number	65,000	75,000	85,000

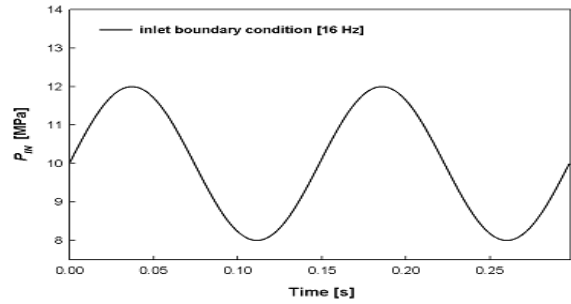


Fig. 15 Inlet boundary condition

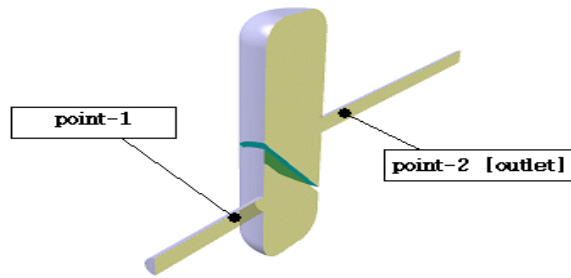


Fig. 16 Measuring points at inlet and outlet pipe

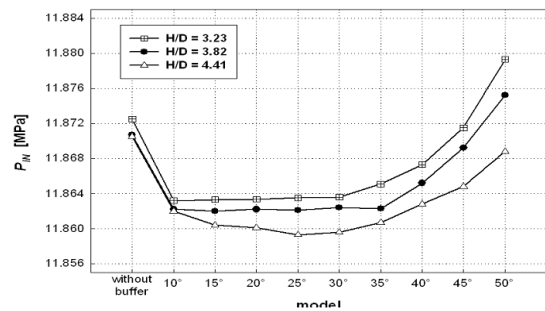


Fig. 17 Mean pressure at point 1

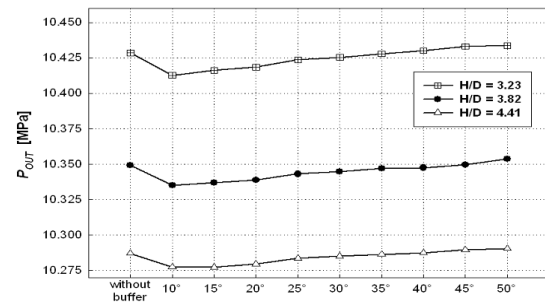


Fig. 18 Mean Pressure at point 2

6. CONCLUSION

The present study has shown the computational fluid dynamics (CFD) can be applied to study pressure characteristics through the snubber.

The numerical analysis on the snubber has been done and gave some information that summarized as follow: The objective in optimizing

a snubber dimension is making the mean pressure loss and pressure pulsation as minimum as possible; The simulation using CFD commercial code with mentioned numerical setting can result a good representation of the real condition. This is proved by the very small difference ratio; The mean pressure both at inlet and outlet pipe show a unique characteristic shown by fig. 17 and 18. The minimum value of mean pressure loss P_{TL} is occurred when buffer angle $\theta = 35$. Decreasing or increasing the buffer angle will increase the mean pressure loss P_{TL} . The minimum value of pressure pulsation P_F is occurred when buffer angle $\theta=10$. Increasing the buffer angle will increase pressure pulsation P_F . The next study should solve the optimization problem not only regarding the minimum mean pressure loss and pressure pulsation but also the minimum volume of snubber.

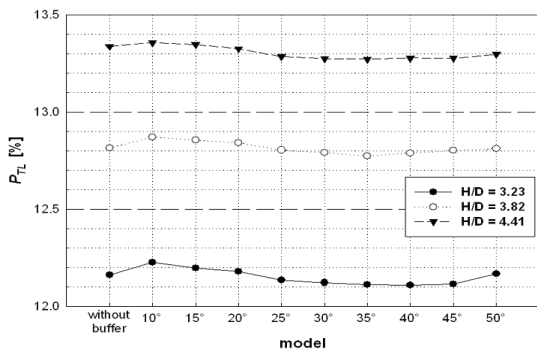


Fig. 19 Pressure loss ratio of all snubber

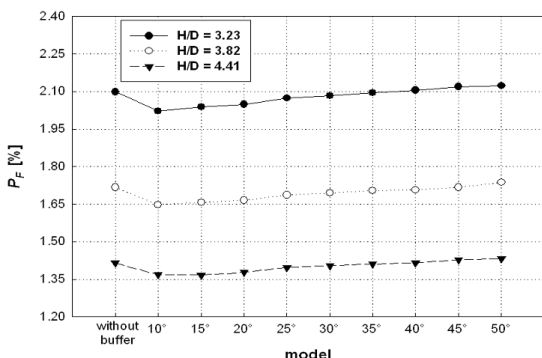


Fig. 20 Pressure pulsation ratio of all snubber

ACKNOWLEDGEMENTS

This research was financially supported by the Ministry of Commerce Industri and Energy (MOCIE), Korea Industrial Technology Foundation

(KOTEF) through the Human Resource Training Project for Regional Innovation and the 2nd-phase of BK21 project of Korea.

REFERENCES

1. Shayegan, S, Hart, D., Pearson, P, and Joffe, D., 2006, "Analysis of the Cost of Hydrogen Infrastructure for Buses in London," Journal of Power Sources, Vol. 65.
2. Heever, S. A, and Grossman I. E., 2003, "A Strategy for the Integration of Production Planning and Reactive Scheduling in the Optimization of Hydrogen Supply Network," Journal of Computers and Chemical Engineering, Vol. 27, pp. 1831~1839.
3. Solovey, V. V., Ivanovsky, A.I, Kolosov, V.I, and Shmal'ko Yu.F, 1995, "Series of Metal Hydride High Pressure Hydrogen Compressors," Journal of Alloys and Compounds, Vol. 231, pp. 903~906.
4. Akbar, W A., Shim, KJ and Yi CS., 2006, "Gas Pressure Fluctuation Characteristics inside Pipe Line Passing through a Snubber for Hydrogen Gas Compressor," Proceeding of International Conference on Sustainable Energy Technologies, Vicenza, Italy.
5. American Petroleum Institute (API), 1995, Reciprocating Compressor for Petroleum, Chemical, and Gas Industry Services, API Standard 618 4th edition, Washington.
6. Methodology Star CD Version 3.24, 2004, CD Adapco Group.
7. B. J. Gim., T. G. Chuah., Fakhru'l-Razi, T. S. Choong., 2005, "The Influence of Temperature and Inlet Velocity on Cyclone Pressure Drop," Elsevier Science B.V., Amsterdam., Vol. 44, No. 1, pp. 7~12.
8. Sobera, M. P. Kleijn, C. R. Brasser, P. van den Akker, H. E. A., 2004, "Multiscale CFD of the Flow, Heat and Mass Transfer through a Porous Material with Application to Protective Garments ," Proceedings, ASME Vol. 149, No. 1, pp. 187~196.
9. J. W. Kim, 2004, "Hydrogen Energy Policy and Technical Trend," The Gas Safety Journal, Special Edition.